New Procedure for Making Schmidt Corrector Plates

Gérard Lemaître

We describe what we call the dioptric elasticity method of making Schmidt plates. An oversize disk is supported on a narrow metal ring. Within this ring, the air underneath is partially evacuated; a primary vacuum is formed under the outer annulus. The elastically deformed disk is worked flat. When the loads are removed, the disk takes on an excellent, smooth Kerber profile over the region interior to the supporting ring. This produces more highly aspherical surfaces ($F/1$) and is more convenient than the method attempted by Schmidt. We give the elasticity theory, discuss our shop methods, and show the very satisfactory results.

Introduction

There are numerous reasons for the present great importance of Schmidt catadioptric systems in their applications to spectrography and the direct study of extended objects.

Within the family of two-mirror anastigmats,[1] the Schmidt telescope (in an idealized, on-axis, all-reflecting form) is incontestably the instrument that possesses—along with the curved-field Schwarzschild telescope—the best compromise between luminosity, physical dimensions, and central obstruction. The Schmidt has, furthermore, the advantage over the Schwarzschild of requiring only one aspheric surface. This surface—theoretically pseudoplane in the two-mirror anastigmat series—is replaced in the catadioptric arrangement (for obvious reasons of obscuration) by an aspheric refracting plate that introduces only slight chromatism. For uv work, it is necessary, for reasons of transparency, that this plate be very thin; we shall see below that with our figuring method it could not be otherwise because the equations of elastic deformation impose this same condition. In the Bouwers or Maksutov systems, the correcting effect of the lens (concentric or afocal, respectively) depends on its thickness. Such cameras are thus distinctly less transparent.

Three-mirror anastigmats (again idealizing the correcting plate by a mirror) of the Schmidt-Cassegrain type,[2,3] although having greater central obstruction, present certain advantages: better accessibility of the focal surface and the possibility of making the field flat by having the Petzval sum equal to zero and also by making one of the two mirrors aspherical. This type of camera is used, for example, on the Mariner probes.[4,5]

Historically, the idea of correcting the aberration of a spherical mirror by use of a refracting plate goes back to Kellner who patented this design in 1910.[6] Later, Schmidt presented this system as a means of achieving small F-ratios. Schmidt seems to have been the first to underline the importance of placing the correcting plate at the center of curvature of the mirror, although Kellner had in fact placed it in this position on his patent drawing. Around 1930 at the Hamburg Observatory, Schmidt succeeded—after several judiciously interpreted experimental trials—in producing corrector plates by a method of elastic deformation.[7]

Research up to now on this difficult problem of working aspherical surfaces suggests numerous methods using thermal expansion, deposit of a variable-thickness coating, abrasion by projection of microparticles, refractive index variation by neutron bombardment, chemical action, geometrical distribution of polishing tool squares, reproduction with cam and pentograph, numerical command arrangements, zonal figuring, elasticity of tools, or elasticity of optics.

The sphere (or the plane) is the surface naturally produced by the wear resulting from rubbing together two indeformable solids of the same dimensions, with a relative movement having three degrees of freedom.

When one wishes to make large size aspheric elements of astronomical quality, one usually uses relatively flexible full size tools, alternating with smaller tools. This method is by far the most widely used, since it has great practical advantages. However, when the flexure of the full-size tool becomes insufficient for wearing away the quantity of glass separating the spherical surface from the surface desired and it becomes necessary to do a good deal of zonal figuring, the small size of the tools used gives rise to discontinuities in the pro-

The author is with the Observatoire de Marseille, 13 Marseille (4), as well as with the Laboratoire d'Astronomie Spatiale, 13 Marseille (12), France.

Received 27 December 1971.

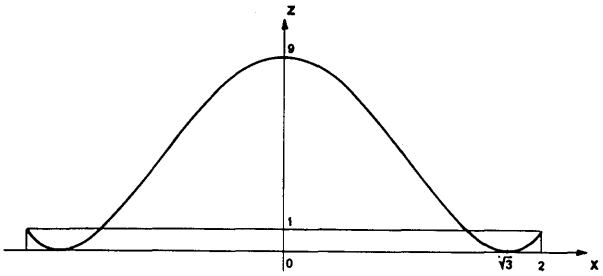

Fig. 1. Kerber profile (nondimensional coordinates).

file. As a result of these discontinuities, there are often circles of stray light around star images in Schmidt photographs, particularly for bright stars.

The new method described here, applicable to correcting plates and thin lenses, uses full-size tools and was developed in order to eliminate such discontinuities and the resultant image defects.

Geometrical Optics

On-axis, and for a given wavelength, a parabolic mirror possesses the same properties as a spherical mirror combined with a refracting plate, the thickness profile of which is such that it introduces into the incident plane wave a retard that is equal to twice the distance separating the parabola from its osculating sphere. This plate is purely divergent with a thickness proportional to the fourth power of the radius. Putting the plate at the center of curvature of the associated spherical mirror, not only is the spherical aberration corrected on axis, but the images are of excellent quality over a much larger field than with a parabola. For other wavelengths this system retains a slight chromatic aberration called the chromatic variation of spherical aberration.

If one accepts the difficulties of making any surface whatever, and in particular, one having inflection points, one can minimize the chromatic effects and obtain a nearly perfect correction for spherical aberration, even for quite large apertures (around $F/1$), with very thin correctors having very weak mean power. Kerber, in his memoir of 1886[8] suggests making the chromatic correction of an objective for the zone of radius $\sqrt{3}H/2$, where $2H$ is the full aperture of the objective. Similarly, the chromatic aberration of a Schmidt plate can be minimized if it is made with a zero power zone called the Kerber zone, at radius $\sqrt{3}H/2$. The result is that, for wavelengths different from that for which the plate is figured (the effective wavelength), the chromatic effect is greatest for the zones of radii $H/2$ and H, and the corresponding deviations have the same value but opposite sign. In this case, if one considers the focal plane defined by the light of the effective wavelength, the extreme colors—arising from equal but opposite variations of index—produce coincident spots that form the circle of least confusion.

Let r be the radius of curvature of the mirror, H the pupil height, n the refractive index of the plate for the effective wavelength, and x the height of the ray considered. The vertex of the corrector surface coincides with the center of curvature of the mirror. The focal point of the combination is the same as that defined by the Kerber zone of the mirror alone.

Let $\Omega = r/4H = F/D$ be the F-ratio of the system and also let $\rho = x/H$ be the reduced radius for an incident ray. If we suppose $\Omega^2 \geq 2$, we make only a slight error in the most unfavorable case in expressing the profile of the plate as[9]

$$Z_{\text{Sch}} = \frac{1}{4^4(n-1)\Omega^3}\left(\tfrac{3}{2}\rho^2 - \rho^4\right)\cdot H, \qquad (1)$$

$$0 \leq \rho \leq 1.$$

In third-order theory, this polynomial is called the Kerber profile (see Fig. 1).

Elasticity

We shall first describe, briefly, Schmidt's experimentally developed method. A plane-parallel plate of thickness h is supported around the edge by the optically flat rim of a sort of bowl that can be rotated. The two surfaces are put into good contact, and the volume under the plate is partially evacuated, with pressure p. If p_0 is the atmospheric pressure, the plate is subjected to a uniform load $q = p_0 - p$. It is elastically deformed by this load, the deformation from a plane surface tangent at the center being given by

$$Z_{\text{Elas}} = \frac{3(1-\nu)}{16}\frac{q}{E}\left(\frac{H}{h}\right)^3\left(2\frac{3+\nu}{1+\nu}\rho^2 - \rho^4\right)\cdot H, \qquad (2)$$

$$0 \leq \rho \leq 1,$$

where E and ν are the Young's modulus and the Poisson's ratio, respectively, of the glass used.

The accessible surface of the plate is ground and polished using a convex spherical tool. If R is the radius of curvature and setting $\varpi = H/2R$, the equation of the just polished surface—still deformed by pressure—is now that of the sphere:

$$Z_{\Sigma} = \varpi(\rho^2 + \varpi^2\rho^4)\cdot H, \qquad (3)$$

$$0 \leq \rho \leq 1.$$

If, now, we remove the plate from the partially evacuated bowl, the bottom surface will revert to a plane, but the top surface will become aspherical. Thus we will obtain a Kerber profile if

$$Z_{\text{Sch}} - Z_{\text{Elas}} + Z_{\Sigma} = 0. \qquad (4)$$

By identifying the coefficients in ρ^2 and ρ^4 in Eq. (4) and setting then each equal to zero, we can eventually solve for the two parameters, R and h, that are at our disposal. For ϖ, we find the following third-degree equation:

$$4^5\frac{3+\nu}{1+\nu}\varpi^3 + 4^5\frac{1}{2}\varpi - \frac{21+5\nu}{(1+\nu)(n-1)}\frac{1}{\Omega^3} = 0.$$

This equation always has a unique and positive real root. This root is very much smaller than unity since

$\Omega^2 \geq 2$; consequently ϖ^3 is negligible ($0 < \nu < 1/2$). This is equivalent to saying that the coefficient of ρ^4 in the development of the sphere is negligible relative to the coefficient of ρ^4 for the elastic deformation.

Since $r = 8\varpi\Omega R$, the radius of the spherical tool can be expressed as a function of the radius r of the mirror,

$$R = \frac{64(1+\nu)(n-1)}{21+5\nu}\Omega^2 \cdot r. \tag{5}$$

For example, if $\nu = 1/5$ and $n = 3/2$, $R \simeq 1.745\,\Omega^2 r$.

Knowing ϖ, we deduce the thickness of the plate,

$$h = \left[\frac{3}{8}(1-\nu^2)(n-1)\frac{q}{E}\right]^{\frac{1}{3}} \cdot r. \tag{6}$$

Relations (5) and (6) define completely the execution conditions. A rapid calculation of maximal tensile stresses shows the desirability of choosing a maximum load q (i.e., 1 atm, with a full vacuum under the plate) if one wants to obtain greatly aspheric plates, and that rupture of the glass occurs for glass type BSC B1664 at an F-ratio of 1.75 if only one face is figured or for $F/1.40$ if both faces are figured.

With the imperative condition that the supporting rim define a plane to within 0.1 μm, this method has the advantage of not having a zone for which the derived equation of the surface is not formally identical to that required by geometrical optics. We shall see below that if one accepts an unusable zone at the edge, it becomes possible to find a configuration of load and support that results in plates of twice the asphericity possible with the above method. The inconvenience of having to use a different radius tool each time one makes a plate for a different F-ratio can be eliminated since a flat tool is used.[10]

The disk of radius R_2 is supported on a metal ring of radius R_1, which divides the surface into two zones (Fig. 2). A load p_1 is exerted on zone 1 (inner) and a load p_2 in zone 2 (exterior to R_1) by means of partial or total evacuation of the air under each zone. The disk is deformed and is ground and polished flat while under these loads. A peripherical ring connected to the support aids in centering the plate and also assures an airtight seal by means of an O-ring. This sliding O-ring touches neither surface of the plate but only the edge, and exerts negligible force, so that the edge of the plate is free to move transversally.

The differential equation for small deformations w of a thin plate of constant thickness h is that due to Lagrange:

$$D \cdot \nabla^2(\nabla^2 w) - p = 0, \tag{7}$$

where

$$D = Eh^3/12(1-\nu^2).$$

D is the rigidity constant of the plate, and p is the load on the plate. Because of the rotational symmetry, we can use the Laplacian operator ∇^2 in polar coordinates given by

$$\nabla^2 = \frac{\partial^2}{\partial R^2} + \frac{1}{R}\frac{\partial}{\partial R} = \frac{1}{R}\frac{\partial}{\partial R}\left(R\frac{\partial}{\partial R}\right).$$

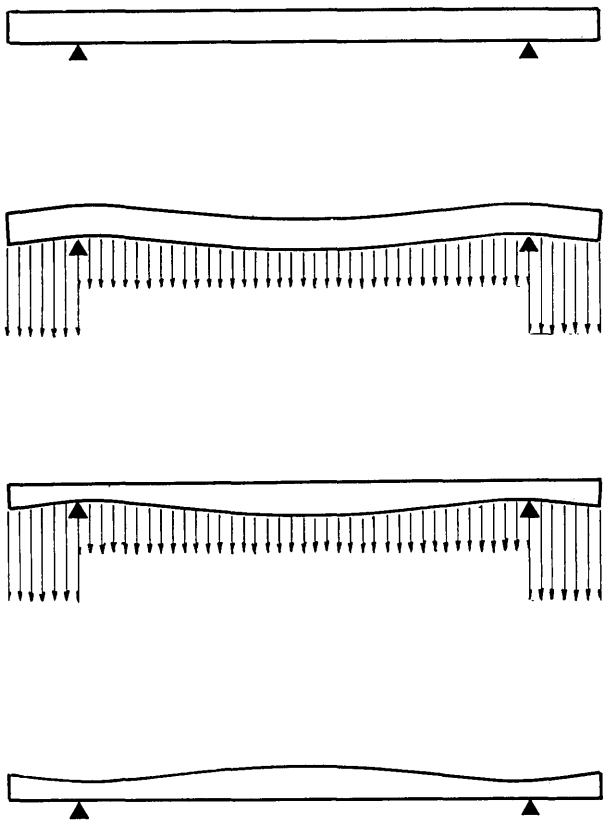

Fig. 2. Principle of the dioptric elasticity method.

Using the reduced radius ρ and reduced deformation Y defined by

$$\rho = R/R_1 \text{ and } Y = (64D/R_1 p_0)w,$$

where p_0 is a constant (ambiant pressure) and defining the reduced operator $\Delta.$ as

$$\Delta. = (1/\rho)(\partial/\partial\rho)[\rho(\partial./\partial\rho)],$$

we see that $\nabla^2 = (1/R_1^2)\Delta.$, and thus Eq. (7) can be written as

$$\Delta(\Delta Y) - 64p/p_0 = 0. \tag{8}$$

Integration of Eq. (8) gives us

$$Y(\rho) = (p/p_0)\rho^4 + C_{\mathrm{I}}\rho^2 \ln\rho + (C_{\mathrm{II}} - C_{\mathrm{I}})\rho^2 + C_{\mathrm{III}} \ln\rho + C_{\mathrm{IV}}. \tag{9}$$

Thus it is necessary to consider two sets of constants C_{I}, C_{II}, C_{III}, and C_{IV}—one set for the interior and one for the exterior zone. In each case, their values are obtained from the boundary and continuity conditions, which are as follows.[11] (The analytic solutions for the inner and outer zones are denoted by Y_1 and Y_2, respectively.)

Boundary conditions:

$$\rho = 0 \begin{cases} \partial Y_1/\partial\rho = 0 & \text{(slope)}, \\ \partial\Delta Y_1/\partial\rho = 0 & \text{(transverse shear stresses)}, \end{cases}$$

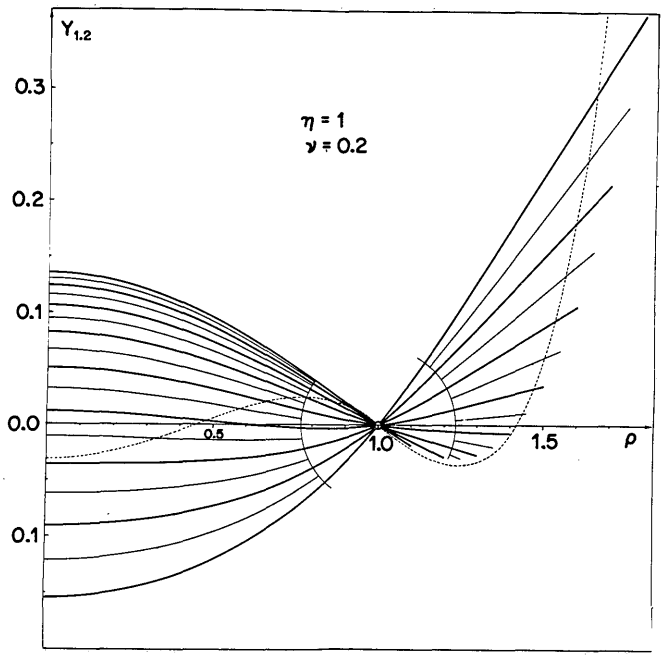

Fig. 3. Grid of profiles for different values of ρ_2 for $\eta = 1$ and $\nu = 1/5$.

$$\rho = \rho_2 \begin{cases} \partial \Delta Y_2/\partial\rho = 0 & \text{(transverse shear stresses),} \\ \partial^2 Y_2/\partial\rho^2 + (\nu/\rho)\partial Y_2/\partial\rho = 0 & \text{(bending couple).} \end{cases}$$

Continuity conditions:

$$\rho = 1 \begin{cases} Y_1 = 0 & \text{(origin of deformations),} \\ Y_2 = 0 & \text{(origin of deformations),} \\ \partial Y_1/\partial\rho = \partial Y_2/\partial\rho & \text{(slope continuity),} \\ \partial^2 Y_1/\partial\rho^2 = \partial^2 Y_2/\partial\rho^2 & \text{(continuity of bending couple).} \end{cases}$$

The two first conditions (at $\rho = 0$) require the constants C_{I} and C_{III} to both equal zero; this results in a biquadratic form for $Y_1(\rho)$ in zone 1.

The loads p_1 and p_2 applied to the plate in zones 1 and 2, respectively, are constants in these zones; we can characterize them by nondimensional parameters q_1 and q_2, where

$$q_1 = p_1/p_0 \text{ and } q_2 = p_2/p_0.$$

The displacements can then be written as

$$Y_1(\rho) = q_1\rho^4 + X_1\rho^2 + X_2, \qquad (10a)$$

$$0 \le \rho \le 1.$$

$$Y_2(\rho) = q_2\rho^4 + X_3\rho^2 \ln\rho + (X_4 - X_3)\rho^2 + X_5 \ln\rho + X_6, \qquad (10b)$$

$$1 \le \rho \le \rho_2.$$

The six constants $X_1, X_2, \ldots, X_6$ depend on three parameters: ν (Poisson's ratio), ρ_2 (i.e., R_2/R_1), and η (i.e., q_2/q_1) which give the geometrical characteristics of the profile. Figure 3 represents the array of Y_1 and Y_2 called $Y_{1,2}(\rho)$ for various values of ρ_2 with $\nu = 1/5$ and $\eta = 1$. The Poisson's coefficient being imposed by the nature of the glass, there is an infinity of pairs (ρ_2, η) that formally satisfies the equation of the Kerber profile for zone 1. By proceding by working the surface flat, one eliminates the inconvenience produced by the execution of a spherical surface by Schmidt's method. The geometrical figure obtained is always a Kerber profile no matter what the thickness is. In fact, the choice of different thicknesses allows one to make correctors for different F-ratio mirrors without changing the apparatus or tools used. However, it is always preferable to make the plate first and then to redetermine the proper curvature of the mirror by carefully measuring the asphericity of the completed plate.

A search for pairs (ρ_2,η) giving Kerber profiles has been made for $0 < \nu < 1/2$. We note that for $\eta = 1$, the surface area of zone 2 (which is not useful) is at a maximum. For $\eta > 1$, the area of zone 2 decreases, and the limiting case—for which η is infinite—requires a plate of zero thickness, excluding all possibility of application. Thus *a fortiori* we chose the compromise $3 \le \eta \le 6$ for large diameter correcting plates.

For each pair (ρ_2, η) giving a Kerber solution, it is necessary to know how the maximal tensile stresses vary as a function of radius in order to be able to compare it to the rupture tensile strength. The radial bending couple can be written as

$$\mathfrak{M}_R = D\cdot\left(\frac{\partial^2 w}{\partial R^2} + \frac{\nu}{R}\frac{\partial w}{\partial R}\right) = \frac{1}{64}R_1 p_0\cdot\left(\frac{\partial^2 Y}{\partial\rho^2} + \frac{\nu}{\rho}\frac{\partial Y}{\partial\rho}\right).$$

Let M be the reduced bending couple such that

$$\mathfrak{M}_R = \tfrac{1}{64}R_1 p_0 \cdot M(\rho).$$

Then

$$M_1(\rho) = 4(3 + \nu)q_1\rho^2 + 2(1 + \nu)X_1,$$

$$0 \le \rho \le 1,$$

$$M_2(\rho) = 4(3 + \nu)q_2\rho^2 + 2(1 + \nu)X_3 \ln\rho + 2(1 + \nu)X_4 + (1 - \nu)X_3 - (1 - \nu)X_5/\rho^2,$$

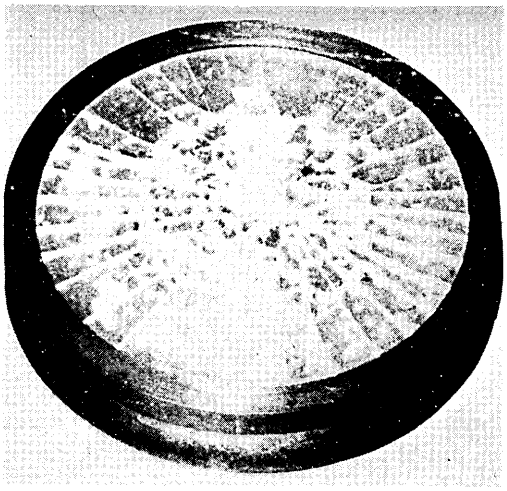

Fig. 4. Rupture pattern of a fused silica disk.

$$1 \leq \rho \leq \rho_2,$$

and the corresponding maximal tensile strength for each zone is

$$\sigma_{1,2}(\rho)_{\text{maxi}} = \frac{3}{32}\left(\frac{R_1}{h}\right)^2 \cdot M_{1,2}(\rho)_{\text{maxi}}.$$

For BSC B1664 glass, one finds that rupture occurs for a corrector for an $F/1.40$ system if one face is figured; if both sides are figured, the limit is $F/1.10$. We have made quartz plates for $F/1$ systems by this method; this represents the limit of possibilities for classical optical materials.

Execution of the Plate

In beginning this work it is preferable to have a small sample of glass available for destructive testing to measure or verify the Young's modulus and the yield stress. For this test one can use a disk supported at the edge and progressively decrease the pressure p underneath, thereby increasing the load. The test plate must of course be thin enough to rupture at a load of less than 1 atm. As p decreases, a measure of the central deflection a gives the Young's modulus since

$$E = \frac{3}{16}(5 + \nu)(1 - \nu)(p_0 - p)\frac{R^4}{ah^3}.$$

As the load is increased, a measure of the pressure just before rupture gives the tensile strength,

$$\sigma_{\text{rupt}} = \frac{3}{8}(3 + \nu)(p_0 - p_{\text{rupt}})\left(\frac{R}{h}\right)^2.$$

Figure 4 shows a sample of fused silica shattered in this manner. Note the excellent homogeneity evidenced by the symmetry of the rupture.

When $\eta \neq 1$ the pressure apparatus can be constituted by the system shown in Fig. 5. A vapor in equilibrium with its liquid at 0°C provides the pressure in zone 1; a primary vacuum is maintained in zone 2.

Small variations of pressure (leaks) or of temperature (heating by polishing) in zone 1 are thus immediately compensated for by the boiling or condensation of a part of the liquid. A cold trap must be placed ahead of the pump to protect against communication between the two zones and especially to purge zone 1 at the beginning. Table I lists liquids useful for this purpose as

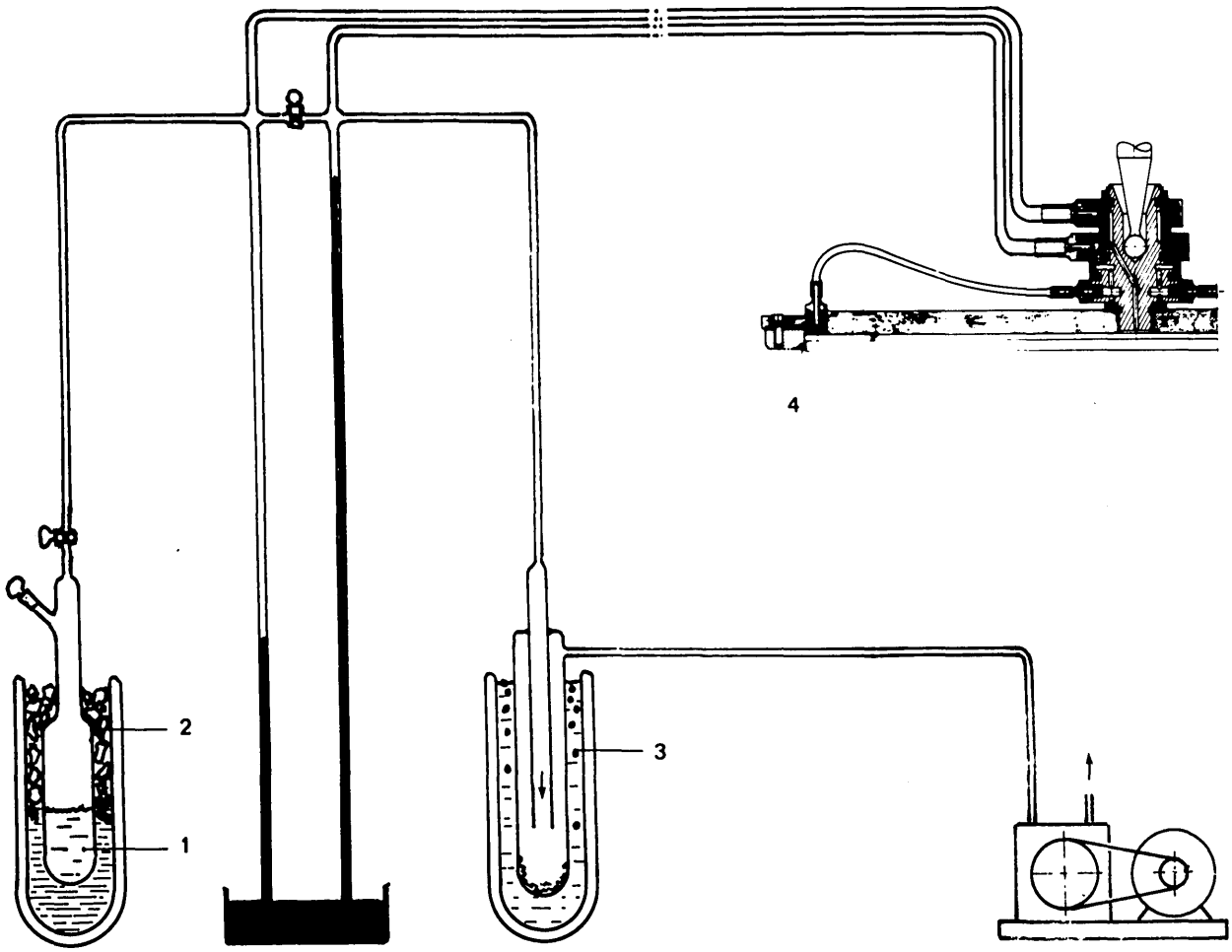

Fig. 5. Pressure apparatus showing (1) liquid in equilibrium with its vapor, (2) ice water, (3) liquid nitrogen, and (4) airtight sliding O-ring.

Table I. Vapor Pressure of Some Compounds at 273 K

Formula	Designation of UIC	p (mm Hg)	η^a
C_2H_4O	Ethane,1,2-epoxy	494.3	2.86
C_4H_2	Butadiyne	518.2	3.15
$CHCl_2F$	Methane, dichloro-fluoro	524.8	3.23
C_5H_{12}	Propane,2,2-dimethyl	529.4	3.29
C_4H_6	1-Butyne	537.2	3.41
CH_5ClSi	Silane, chloromethyl	549.3	3.60
$COCl_2$	Carbonyl, chloride	550.6	3.63
C_2H_7N	Amine, dimethyl	555.2	3.71
C_3H_8O	Ether, ethyl-methyl	561.8	3.83
CH_4S	Methanethiol	569.7	3.99
C_3O_2	Propadiene,1,3-dioxo	588.4	4.46
C_4H_4	1-Buten-3-yne	617.2	5.32
IF_7	Iodine heptafluorine	619.7	5.42
CH_3Br	Methane,bromo	659.8	7.58

[a] $\eta = q_2/q_1 = p_0/(p_0 - p)$ with $p_0 = 760$ mm Hg.

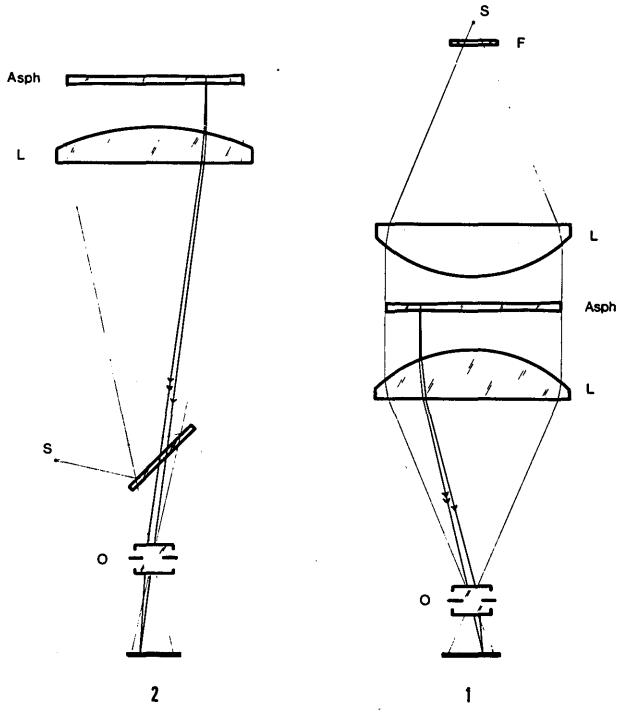

Fig. 6. Interferometric mountings.

calculated from the physical constants[12] using Dupré's formula,

$$\log p = \alpha - \frac{\beta}{T} - \gamma \log T.$$

Mountings 1 and 2 of Fig. 6 permit us to obtain easily the interference fringes of constant thickness between the front and back surfaces of the plate. In mounting 1, it is necessary to semialuminize the two surfaces to enhance the contrast and give narrow fringes (Fig. 7).

For mounting 2 (Fizeau interferometer) a He–Ne laser is used (Fig. 8). These two mountings give excellent reading precision since one fringe represents a deformation of the refracted wavefront of $\lambda(n - 1)/2n \simeq \lambda/6$. The slight wedge in the plate, which is superimposed on the Kerber profile, is much too slight to give rise to a detectable chromatic effect and in no way affects the performance of the Schmidt camera.

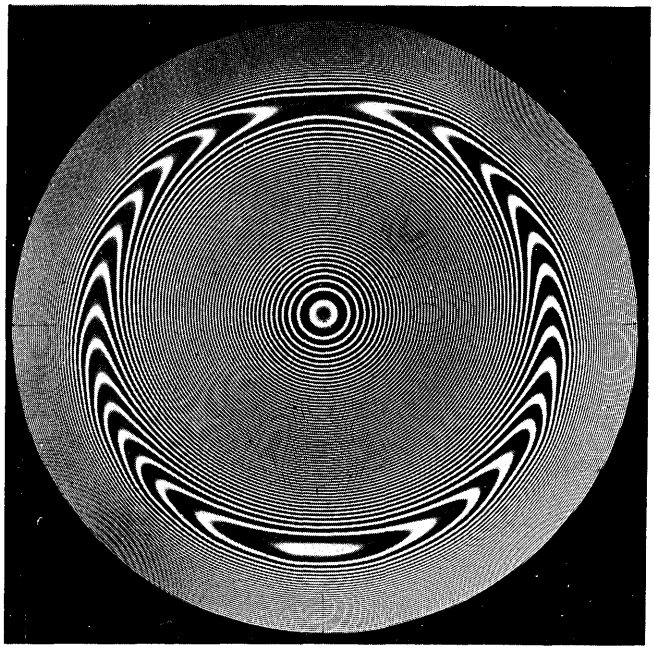

Fig. 7. Fringes of equal thickness (mounting 1) of a plate made by the dioptric elasticity method.

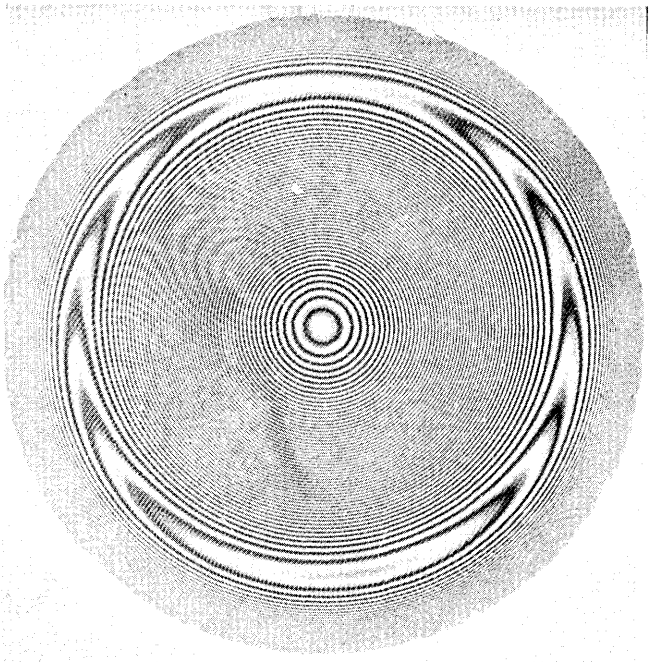

Fig. 8. Fringes of equal thickness (mounting 2) of a plate made by the dioptric elasticity method.

Conclusions

Beside the advantage of a profile as smooth as that of a spherical surface, the dioptric elasticity method gives —for small thickness and at the price of a slight amount of complication in the initial setup—correcting plates or lenses that are highly aspheric ($F/1$) with a fabrication time of the same order of magnitude as for spherical lenses. Although this method has been extremely useful for us in the production of small and medium diameter optics, it was conceived essentially for large aperture plates.[13]

The deformation of both faces is often advantageous, and, when necessary, the two surfaces that are calculated can be corrected in such a way as to cancel out rigorously the effects due to the plates own weight. It is possible to obtain numerous other profiles and to further increase the precision of the deformation by working with an ambiant pressure of several atmospheres. Finally, we note that correctors have been made recently using aspherical plates for improving the off-axis image quality for Newtonian and Cassegrainian foci of large telescopes,[14–17] and that the dioptric elasticity method would seem to be well suited for fabricating such optical components.

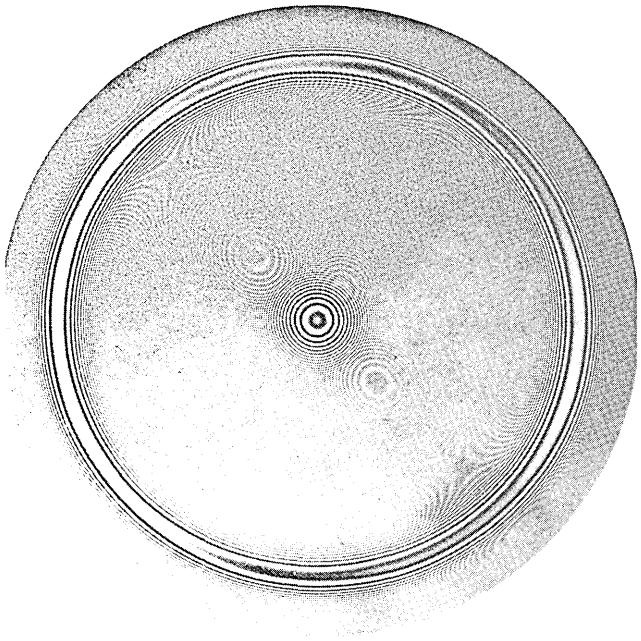

Fig. 10. Fringes of equal thickness of a plate figured to $F/1.1$.

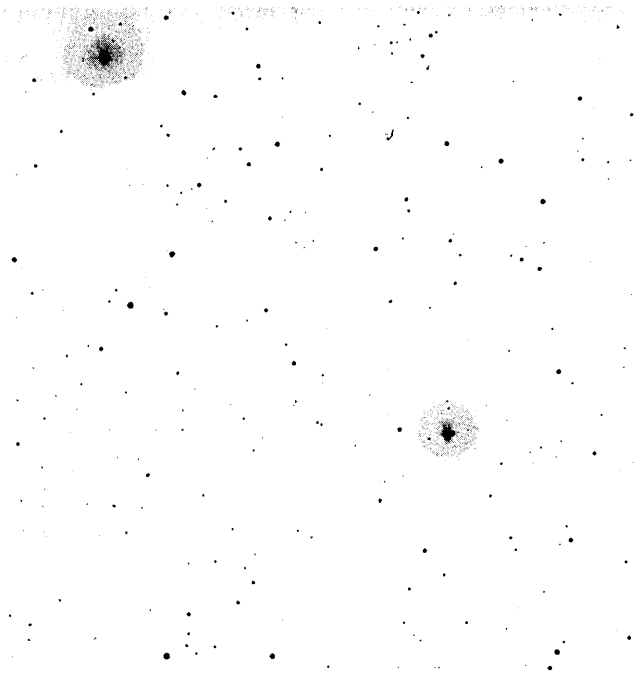

Fig. 9. Region of δ Ori (lower right) $m_v = 2.5$ and ϵ Ori (upper left) $m_v = 1.7$ photographed with a $F/1.5$ Schmidt system. Corrector plate in BSC B1664 of 24-cm aperture produced with a pressure ratio $\eta = 6$. Kodak IIaO, 3 min, no filter. The absence of circles around bright stars attests to the continuity of the surface of the plate.

I wish to thank C. Fehrenbach and A. Baranne who encouraged this project in many ways and who made available the facilities of the Marseille Observatory as well as those of the Haute-Provence Observatory; and G. Courtès who greatly supported this work by making the facilities of the Laboratoire d'Astronomie Spatiale available for the first practical trials. G. Moreaux was responsible for the fabrication of the first plates and greatly aided with many of the initial practical problems.

J. Caplan translated this article into English.

References

1. C. G. Wynne, J. Opt. Soc. Am. **59,** 572 (1969).
2. J. G. Baker, J. Am. Philos. Soc. **82,** 339 (1940).
3. C. R. Burch, Monthly Notices Roy. Astron. Soc. **102,** 159 (1942).
4. D. R. Montgomery and L. A. Adams, Appl. Opt. **9,** 277 (1970).
5. G. Courtes, in *New Techniques in Space Astronomy,* F. Labuhn and R. Lüst, Eds. (International Union of Astronomy, Paris, 1971).
6. American Patent 969,785 (1910).
7. B. Schmidt, Mitt. Hamburger Sternv. **7,** 15 (1932).
8. A. Kerber, Central Zeit, f. Opt. und Mech. p. 157 (1886).
9. H. Chrétien, *Calcul des combinaisons optiques* J. & R. Sennac, Eds. (1959) p. 349.
10. G. Lemaître, D. E. A., Fac. Sc. Marseille (unpublished) (1968); Compt. Rend. **t. 270A,** 226 (1970).
11. G. Lemaître, ESO Bull. No. 8, 21 (1971).
12. D. E. Gray, Ed., *American Institute of Physics Handbook* (McGraw-Hill, New York, 1963).
13. French Patent, ANVAR 70,19,261 (1969).
14. S. C. B. Gascoigne, The Observatory **85,** 79 (1965).
15. D. H. Schulte, Appl. Opt. **5,** 309 (1966).
16. A. Pourcelot, Compt. Rend. **t. 262B,** 982 (1966).
17. H. Köhler, ESO Bull. No. 2, 13 (1967).